NASA Technical Paper 1527

# Optically Isolated Logarithmic Nanoammeter Capable of Floating to 5 Kilovolts

John C. Sturman and John C. DeLaat

OCTOBER 1979

NASA

NASA Technical Paper 1527

# Optically Isolated Logarithmic Nanoammeter Capable of Floating to 5 Kilovolts

John C. Sturman and John C. DeLaat
*Lewis Research Center*
*Cleveland, Ohio*

National Aeronautics
and Space Administration

**Scientific and Technical
Information Branch**

1979

## SUMMARY

A logarithmic current-measuring instrument has been developed that can operate at a common-mode voltage of 5 kilovolts. Positive or negative currents can be measured from $10^{-9}$ to $10^{-3}$ ampere direct current. Optical isolation is used to control input switching and to provide data referenced to ground potential. Analog meter readouts as well as 0- to 5-volt outputs are provided for peripheral data collection. Six independent channels are provided: Three measure positive currents, and three measure negative currents.

This instrument was designed to measure plasma coupling currents as part of the spacecraft environmental interaction studies at the Lewis Research Center. Although designed for vacuum operation, it can be used equally well in air to measure low currents at high common-mode voltages.

## INTRODUCTION

In the future, spacecraft will be larger and will necessarily require higher electric power levels for their operation. As the power is increased, solar-array voltages will have to be increased from the current low voltage (28 to 32 V) to hundreds or even thousands of volts in order to keep distribution losses reasonable. At these higher voltages, even very small exposed conductor areas can collect sizable currents from the space plasma environment. Where insulating surfaces are present, plasma-initiated discharges can also occur. These effects cause power losses, surface degradation due to arcing, and electrical interference.

High-voltage surface-plasma interactions (refs. 1 to 6) have been studied at the Lewis Research Center for the past several years. This study includes both laboratory (refs. 7 to 9) and satellite experiments (refs. 10 to 13). Both experimental programs require a means of measuring currents coupled to a plasma from surfaces biased to voltages between 1 and 15 kilovolts. Any such instrument must be capable of measuring currents from nanoamperes to milliamperes and must be able to survive the plasma discharges that occur at these high voltages. Designing an instrument to meet these requirements poses a number of problems.

If the current-measuring instrument is placed in the ground lead of the high-voltage supply, the current to be measured is not easily distinguished from leakage

currents. If the current-measuring instrument is placed in the high-voltage supply load, it can measure the correct current, but it must float at the full high voltage. This requires both a high-voltage, isolated power supply to power it and some means of coupling its output down to ground reference. A current meter that could be floated to 16 kilovolts was developed for the SPHINX satellite (ref. 13) and was later used on the PIX flight experiment (refs. 10 and 11). Currents from $10^{-9}$ to $10^{-4}$ ampere could be measured at common-mode voltages up to 16 kilovolts. It worked well but was complex and expensive and had large calibration shifts with temperature. The instrument described herein is simple and inexpensive and requires minimal temperature compensation. Though the instrument has been built for laboratory use at voltages to ±5 kilovolts, it can easily be modified for higher voltage operation at minimal cost and complexity.

## DESIGN REQUIREMENTS

This instrument was designed to make wide-range coupling current measurements in a plasma environment at voltages to 5 kilovolts. It is required to measure direct currents from $10^{-9}$ to $10^{-3}$ ampere, to operate in vacuum, and to be remotely controlled. The operating temperature was specified as $-40^{\circ}$ to $60^{\circ}$ C, and the desired accuracy is ±10 percent of reading. The instrument must survive overcurrents and transients caused by the biasing supply arcing to ground. In some cases this could result in a 5-kilovolt pulse being applied directly across the nanoammeter input. Complete specifications for the nanoammeter are given in table I.

Each instrument has six independent current channels: three for positive current, and three for negative current. Each channel can be switched between its input and a built-in calibrating current source. Instrument output was chosen to be logarithmic in order to provide six decades of current measurement in one range. This eliminates the complexity of autoranging and the requirement for a range information output.

Separate units are used for positive and negative currents. One three-channel unit of each kind is controlled and read out by the control panel, which displays one positive and one negative channel on two log meters. Analog 0- to 5-volt outputs referenced to ground potential are also provided for all six channels.

Because in this application it was expected that the negative coupling currents would be somewhat higher than the positive, the current ranges were made unequal. The negative unit measures $-5\times10^{-9}$ to $-5\times10^{-3}$ ampere; the positive unit measures $1\times10^{-9}$ to $1\times10^{-3}$ ampere. Each unit consists of a floating high-voltage section that is signal isolated by opto-isolators and can be operated 5 kilovolts above or below the low-voltage section, which is referenced to ground potential. Power is furnished by

commercial, high-voltage, isolated supplies. Power consumption is kept low to minimize heat-dissipation problems in vacuum. Each of the two units requires 2.5 watts at 28 volts direct current and is 15.7 centimeters long by 15.7 centimeters high by 11.9 centimeters wide (6.2 in. by 6.2 in. by 4.7 in.).

A significant factor in achieving low-power operation was the use of latching reed relays at the inputs. These are special low-leakage versions of a standard relay. They are magnetically latching and require no power except when switching.

One complete six-channel system is shown in figure 1, and one set of circuit cards in figure 2. Three of the four printed circuit cards are mounted in the upper, isolated section of the instrument. These are the relay card; the analog circuits card; and the opto-isolator card, which also includes the high-voltage, isolated power supply. The single output card is mounted in the lower section of the unit. All cards measure 11.5 centimeters by 15.24 centimeters (4.5 in. by 6 in.).

## CIRCUIT DESCRIPTION

A block diagram of the signal path for one channel is shown in figure 3. Each of the three channels in a unit is independent and can be switched through the input latching relays (K1A to K3B) to either its input terminal or a calibration source that provides a 5-microampere current (±1 percent). The exact configuration is shown on the relay card schematic (fig. 4).

Input protection against arcs or other transient overloads is provided in two steps. On the relay card (fig. 4) a 0.001-microfarad feedthrough capacitor and a 90-volt-breakdown gas surge suppressor are connected between input and common. After the relay card, a series-resistor - shunt field-effect transistor (FET) diode combination on the analog circuits card (fig. 5) clamps the input to the plus-or-minus 12-volt supply. Fourteen-volt zener diodes placed across the supplies close to the input provide protection against externally induced supply-voltage transients.

A current inverter (U1) is required for measuring negative current because the following log amplifier accepts only positive current. The inverting stage has a gain of -1/3 over the full six-decade current range. Less-than-unity gain extends the maximum current range.

The current inverter circuit can be operated over the full six decades because the current-voltage characteristic of the quad transistors used is logarithmic. This feature insures practical voltage levels at all currents. Three of the transistors are connected in parallel as diodes in the input feedback circuit; the fourth is connected as a diode in the stage output. If the voltage drop across the diodes is maintained equal by operational amplifier U1, currents through all identical diodes will be equal. In this

way the output will be one-third of the input and will be positive for a negative input. Operational amplifier U1 has sufficiently low input current and low offset voltage that no trimming is required. For measuring positive currents, the current inverter stage is omitted and the input is taken directly into the next stage.

The second stage uses a monolithic log amplifier (U2) that transforms the input current to be measured into a voltage with a scale factor of about 0.9 volt per decade. This particular integrated circuit provides the log circuit and the necessary temperature compensation on one chip, which considerably improves temperature tracking over previous discrete-component log circuits. It is a fairly old device and the minimum input current is limited by the leakage of the input FET amplifier, particularly at high temperatures.

The last stage of this card is a monolithic voltage-to-frequency (V-to-F) converter. Its input stage is biased from a stable reference in order to compensate for the output offset of the log stage. It is trimmed to produce a 10-kilohertz output at full-scale input current and zero frequency at a minimum input of $1\times10^{-9}$ or $-5\times10^{-9}$ ampere.

Outputs from the V-to-F converters are wired to the opto-isolator card (fig. 6). Buffering is provided by a pair of parallel 74C14 gates (U1) that drive the opto-isolator. Approximately half of the opto-isolator card is at high voltage, the other half is at ground potential. The card layout provides a 1.27-centimeter (1/2-in.) space between the high- and low-voltage sections. On the low-voltage side of the card, the frequency signal from the opto-isolator is compared with a 1.8-volt reference by U7 and provides a clean output with well-defined rise and fall times. The high-voltage isolated power supply that powers all circuits operating off ground potential is also mounted on the opto-isolator card. It is the only card that has both high and low voltage on it.

On the output card (fig. 7) are three frequency-to-voltage (F-to-V) converters. They use the same integrated-circuit V-to-F converters as a high-linearity voltage-controlled oscillator in a phase-locked loop (U3, U4, and U5). It can lock to any frequency from 0 to 10 kilohertz and responds in three or four cycles to a step change of input frequency. Exclusive NOR gate U1 is used as the phase comparator in the phase-locked loop. The circuit produces a 0- to 5-volt output that is buffered by operational amplifiers U6, U7, and U8 and is connected by cable to the control panel. The output card also contains a simple switching regulator that converts the 28-volt dc primary power to 10 volts so that it will operate all the ground-referenced circuitry. At the control panel (fig. 8), the analog signals are again buffered by unity-gain amplifiers U1, U2, and U3. One of the three analog outputs is also switch selectable for display on a meter.

## CONTROL CIRCUITS

The remainder of the circuitry is required to control the six input relays in each unit. To minimize the number of interconnecting wires and opto-isolator channels, a pulse-time coincidence circuit is used. Only two lines are required to control 12 functions, that is, on-and-off signals for six pairs of relays. The control block diagram in figure 9 shows how this works. Two identical shift registers, one on the high-side relay driver card and the other in the control panel, are synchronized to operate together. Synchronization is insured by operation from a common clock containing a wide pulse every 32 pulses that is used to reset the registers. Each shift register has an identical wide-pulse detector that resets it to zero and initializes it with a 1 in the first bit position. The 1 advances in step through successive stages of both registers. When one of the control switches is closed, a pulse appearing at that output will be placed on the control line, optically isolated, and applied to the decoding gates on the relay driver card. A corresponding output of the high-side shift register will also be high at this time. The coincidence of these two pulses is detected by the NAND gate connected to that particular shift-register output line and drives the corresponding relay function. If a different switch is closed, coincidence will occur on a different line at a different time to control a different output.

The complete schematic for the control-panel switching circuits is shown in figure 10. The corresponding high-side circuits are on the relay driver card (fig. 4). The clock is generated by the top line of circuits in figure 10. A stable multivibrator (U1A, U1B) generates 1.8-millisecond-wide pulses with a 15-millisecond period that drives counter U3. At every 32nd pulse its output goes high, driving a differentiator and a Schmitt trigger (U2C) to produce a 5-millisecond pulse. This is the wide pulse that is added to the clock in gate U4A, which functions as a negative input NOR. Its output is buffered by Q1 and drives the clock lines ($C_L$) to the opto-isolators. The signal is also inverted by U2D, which drives the wide-pulse detector circuit and clocks the shift register. The one wide pulse is detected by Schmitt trigger U2E and its input network. The output of U2D is normally high and causes the output of U2E to be low. During a clock pulse, U2D pin 8 goes negative and discharges the 2200-picofarad capacitor (C3) through 1.8 megohms. This RC time constant is set so that the input must be low for 3 milliseconds to discharge C3 to the lower trigger point of the Schmitt trigger. Therefore, U2E only produces an output on the 5-millisecond-wide pulse. This output directly resets the shift register to the zero state and is also differentiated to produce an 18-millisecond pulse that sets the first stage of shift register U5 to a 1 on the next clock pulse. Successive clock pulses advance the single 1 state through the register. If one of the switches connected to the shift register output is closed, the

pulse is gated to the $S_L$ output line, optically isolated, and transferred to the high-side electronics.

On the relay card, the pulse on the S line is in time-coincidence with the shift register output corresponding to the one switch closure that generated it. This is detected by a single NAND gate. Each gate output connects to a relay driver that applies either 12 or -12 volts to the input latching relays. The two SPST relays are connected in inverse parallel through isolating diodes so that a signal that latches one on will unlatch the other, and conversely. Diode isolation is required to prevent the stored energy from the much larger high-voltage relay from reverse latching the smaller calibrate relay when the drive pulse is removed. There is one pair of relays for each channel. When the low-side shift register pulse is selected, it is also used to latch a 4013 flip-flop (U9, U10, and U11) that indicates what function was selected by lighting a lamp in the corresponding switch.

## VERIFICATION AND TESTING

To date, one complete nanoammeter instrument has been built, that is, one positive and one negative unit with three channels each and one control panel. Both the positive and negative units, were operated in a temperature chamber at $-40^{\circ}$ to $60^{\circ}$ C. A typical pair of calibration curves is shown in figure 11. Log conformity at any given temperature is excellent, but there is a definite gain change with temperature.

The nanoammeters will probably be operated over a more limited temperature range. Taking $\pm 40^{\circ}$ C as the temperature extremes, the maximum error is within $\pm 15$ percent of reading from the best straight line except at the extremes of current. This is with no attempt at temperature compensation and is sufficiently accurate for its intended use. For many other applications the temperature would be known and a correction factor could be applied.

## DISCUSSION

Analysis of the test data shows that the predominant error in calibration appears as an increased circuit gain with increasing temperature. There are several possible causes for this, the most probable being the temperature coefficient of the timing capacitors in the V-to-F and F-to-V converters, the log amplifier, and the current inverter stage. Previous work on a similar instrument that did not use a voltage-to-frequency converter showed similar temperature shifts. In that case the shift was traced to the ICL 8048 log amplifier. Considerable difference has been found in 8048's from different lots, and even within one lot. It is therefore recommended that the 8048

log amplifiers be selected for applications requiring high accuracy over a wide temperature range. Alternatively, the performance of similar circuits using the 8048 has been improved by using temperature-compensating resistors in the analog signal output path. Both silicon resistors and Corning nickel film resistors have been used successfully.

## CONCLUSIONS

Operation of a six-channel, high-voltage, isolated nanoammeter capable of operation at common-mode voltages to ±5 kilovolts in vacuum has been demonstrated. The instrument is simpler and less expensive than its predecessors, uses half the power, and requires minimal temperature compensation. Although intended for laboratory use, the design could easily be adapted for flight applications. The main limitation is the 5-kilovolt maximum isolation. This could easily be increased to 15 kilovolts by using either fiber optics or an open transmission path for the optical isolation. Isolated power supplies for operation at 15 kilovolts are also available. Minimal redesign of the circuits would be required for higher isolation voltage and should not greatly increase the cost.

Lewis Research Center,
National Aeronautics and Space Administration,
Cleveland, Ohio, May 30, 1979,
506-23.

## REFERENCES


1. Knauer, W.; et al.: High Voltage Solar Array Study. (Hughes Research Labs.; NASA Contract NAS3-11535.) NASA CR-72675, 1970.
2. Springgate, W. F.; and Oman, H.: High Voltage Solar Array Study. (D2-121734-1, Boeing Co.; NASA Contract NAS3-11534.) NASA CR-72674, 1969.
3. Cole, R. W.; Ogawa, H. S.; and Sellen, J. M., Jr.: Operation of Solar Cell Arrays in Dilute Streaming Plasmas. (TRW-09357-6006-R000, TRW Systems; NASA Contract NAS3-10612.) NASA CR-72376, 1968.
4. Herron, B. G.; Bayless, J. R.; and Worden, J. D.: High Voltage Solar Array Technology. AIAA Paper 72-443, Apr. 1972.
5. Kennerud, K. L.: High Voltage Solar Array Experiments. (Boeing Aerospace Co.; NASA Contract NAS3-14364.) NASA CR-121280, 1974.

6. Fralick, G. C.: Calculation of Current Collected in a Diluted Plasma Through a Pinhole in the Insulation Covering a High Voltage Surface. NASA TN D-7957, 1975.

7. Domitz, S.; and Grier, N. T.: The Interaction of Spacecraft High Voltage Power Systems with the Space Plasma Environment. Power Electronics Specialists Conference. Institute of Electrical and Electronics Engineers, Inc., 1974, pp. 62-69.

8. Grier, N. T.; and Domitz, S.: Current from a Dilute Plasma Measured Through Holes in Insulators. NASA TN D-8111, 1975.

9. Stevens, N. J.; et al.: Investigation of High Voltage Spacecraft System Interactions with Plasma Environments. AIAA Paper 78-672, Apr. 1978.

10. Grier, N. T.; and Stevens, N. J.: Plasma Interaction Experiment (PIX) Flight Results. Spacecraft Charging Technology - 1978. NASA CP-2170, 1979.

11. Ignaczak, Louis B.; et al.: The Plasma Interaction Experiment (PIX) - Description and Flight Qualification Test Program. AIAA Paper 78-674, Apr. 1978.

12. Stevens, N. J.: Space Environmental Interactions with Spacecraft Surfaces. Presented at the 17th AIAA Aerospace Sciences Meeting, New Orleans, La., Jan. 15-17, 1979. (Also NASA TM-79016, 1979.)

13. Stevens, N. J.: Solar Array Experiments on the SPHINX Satellite. NASA TM X-71458, 1973.

TABLE I. - SPECIFICATIONS FOR OPTICALLY ISOLATED LOGARITHMIC NANOAMMETER

| | |
|---|---|
| Current range, A: | |
| Positive | $1\times10^{-9}$ to $1\times10^{-3}$ |
| Negative | $-5\times10^{-9}$ to $-5\times10^{-3}$ |
| Floating voltage (maximum), kV | ±5 |
| Input protection, kV | ±5 |
| Accuracy (temperature compensated), percent | ±5 |
| Operating temperature, °C | -40 to 60 |
| Temperature drift (compensated), percent/deg C | <0.15 |
| Internal calibrator accuracy, percent | ±1 |
| Number of channels: | |
| Positive | 3 |
| Negative | 3 |
| Power required,[a] V ac ± percent | 120±20 |
| Size, cm (in.): | |
| Sensing units | 15.7 × 15.7 × 11.9 (6.2 × 6.2 × 4.7) |
| Control panel | 13.33 ($5\frac{1}{4}$) high by 48 (19) rack mount |
| Maximum distance between units and control, m (ft) | >15 (50) |
| Readout,[b] V dc | 0 to 5 |
| Environment | Vacuum or air |

[a]Control panel provides 2.5 W at 28 V dc to each unit.

[b]Logarithmic panel meters plus analog voltage output.

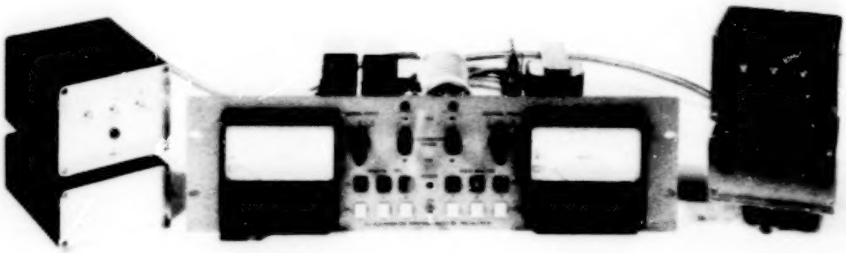

C-79-409

Figure 1. - Floating nanoammeter system.

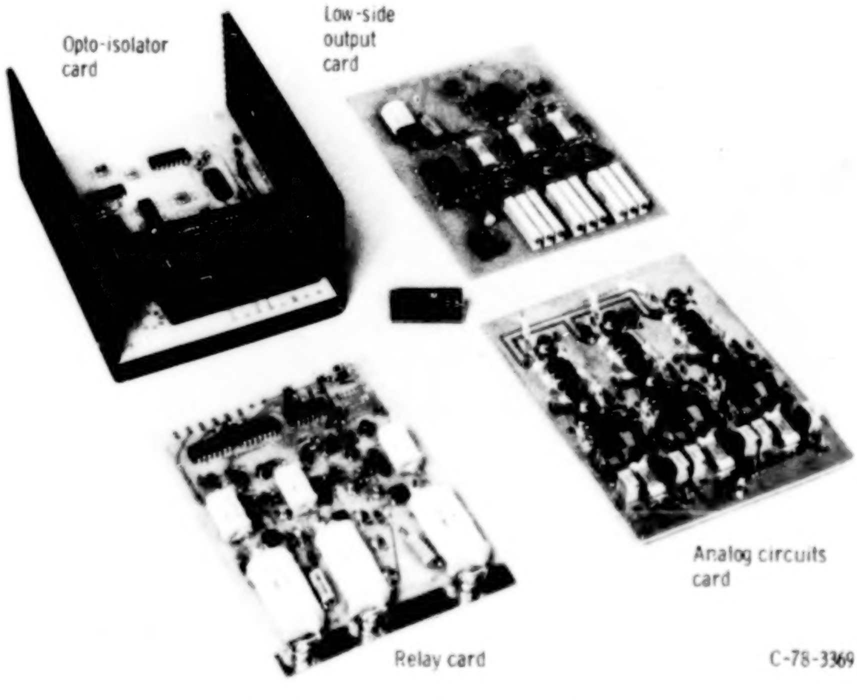


Figure 2. - Nanoammeter circuit cards.

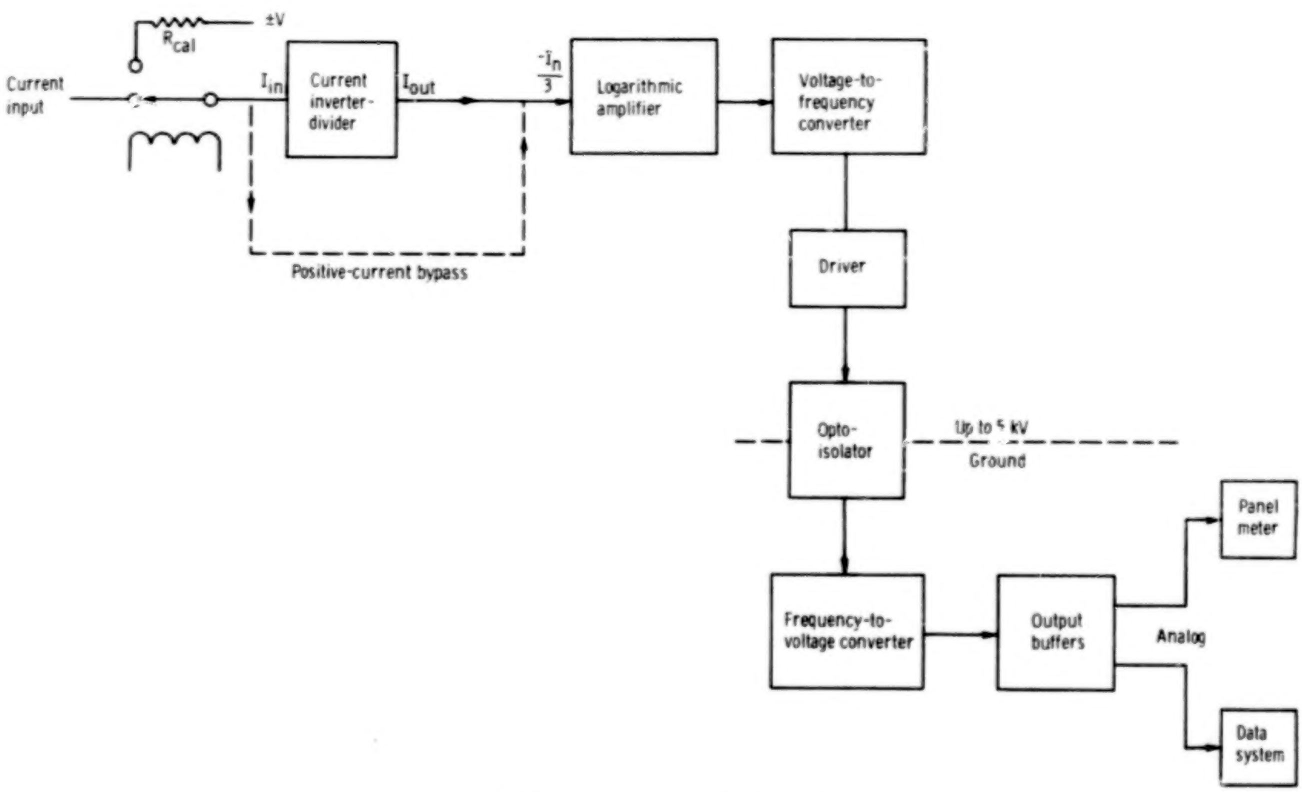


Figure 3. - Optically isolated nanoammeter signal block diagram.

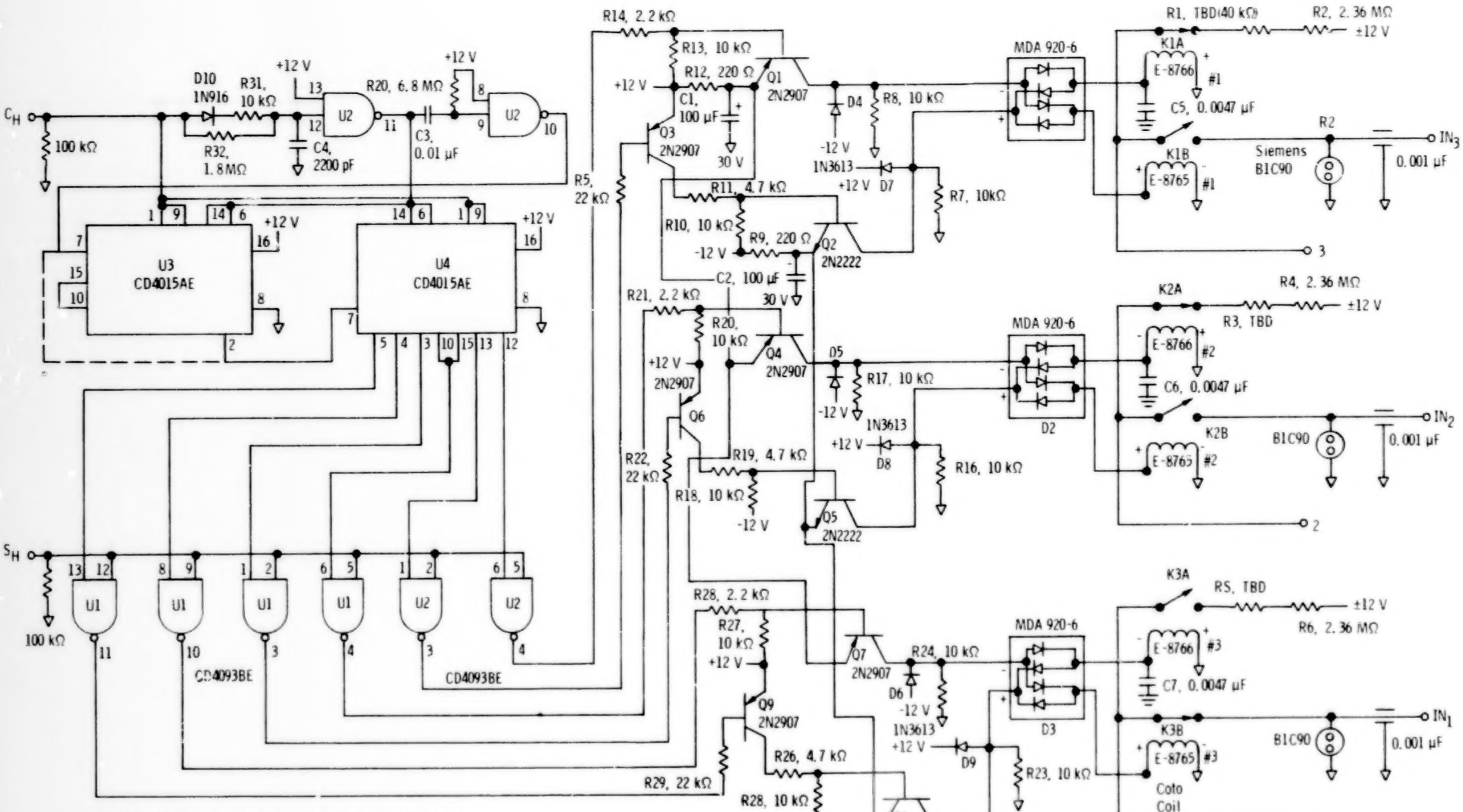


*Delete U3 and install dotted jumper for negative input unit.

Figure 4. - Optically isolated nanoammeter relay card.

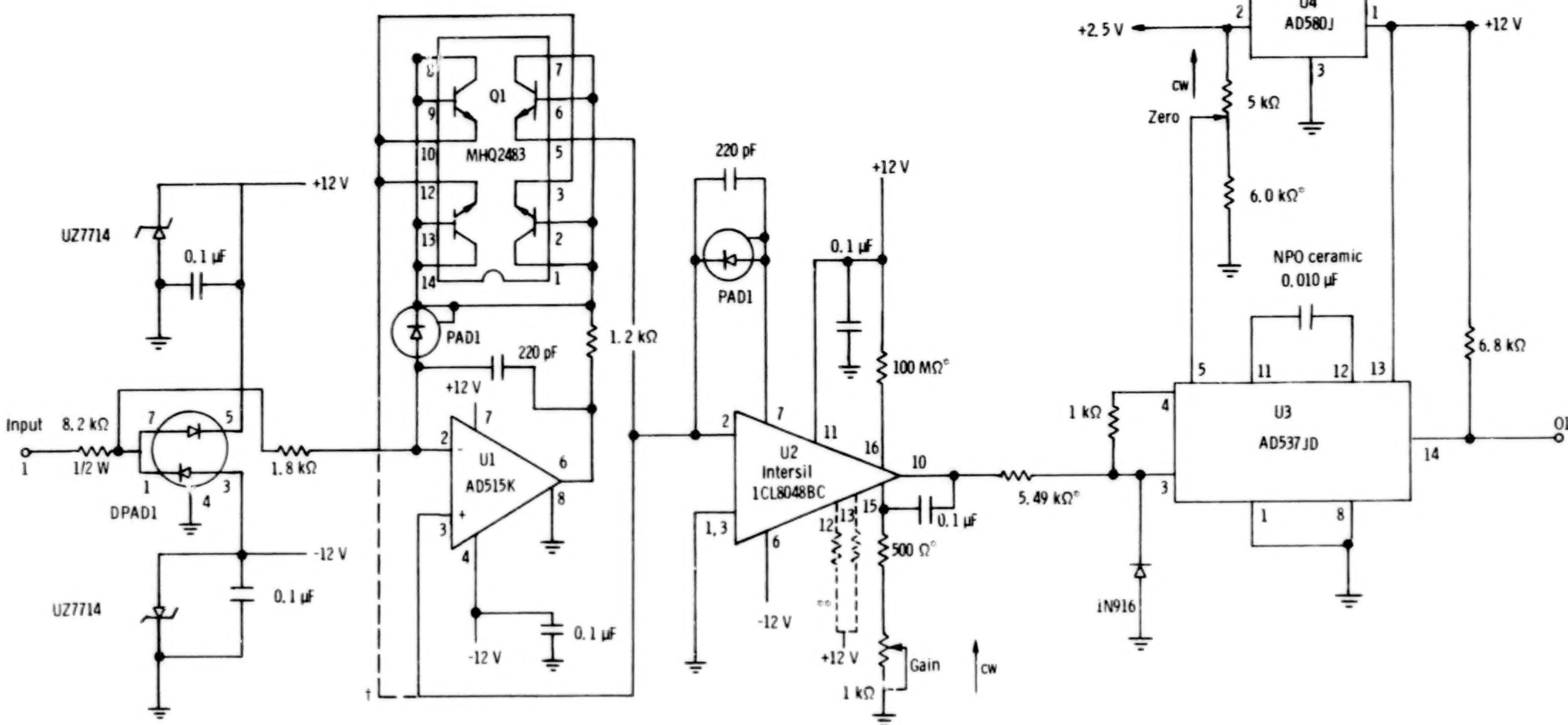


° Metal film.

°° Use one resistor of pair for offset trim.

† For positive input, add dotted jumper and omit components betwen 1.8-kΩ resistor and 8048.

Figure 5. - Optically isolated nanoammeter analog circuits card.

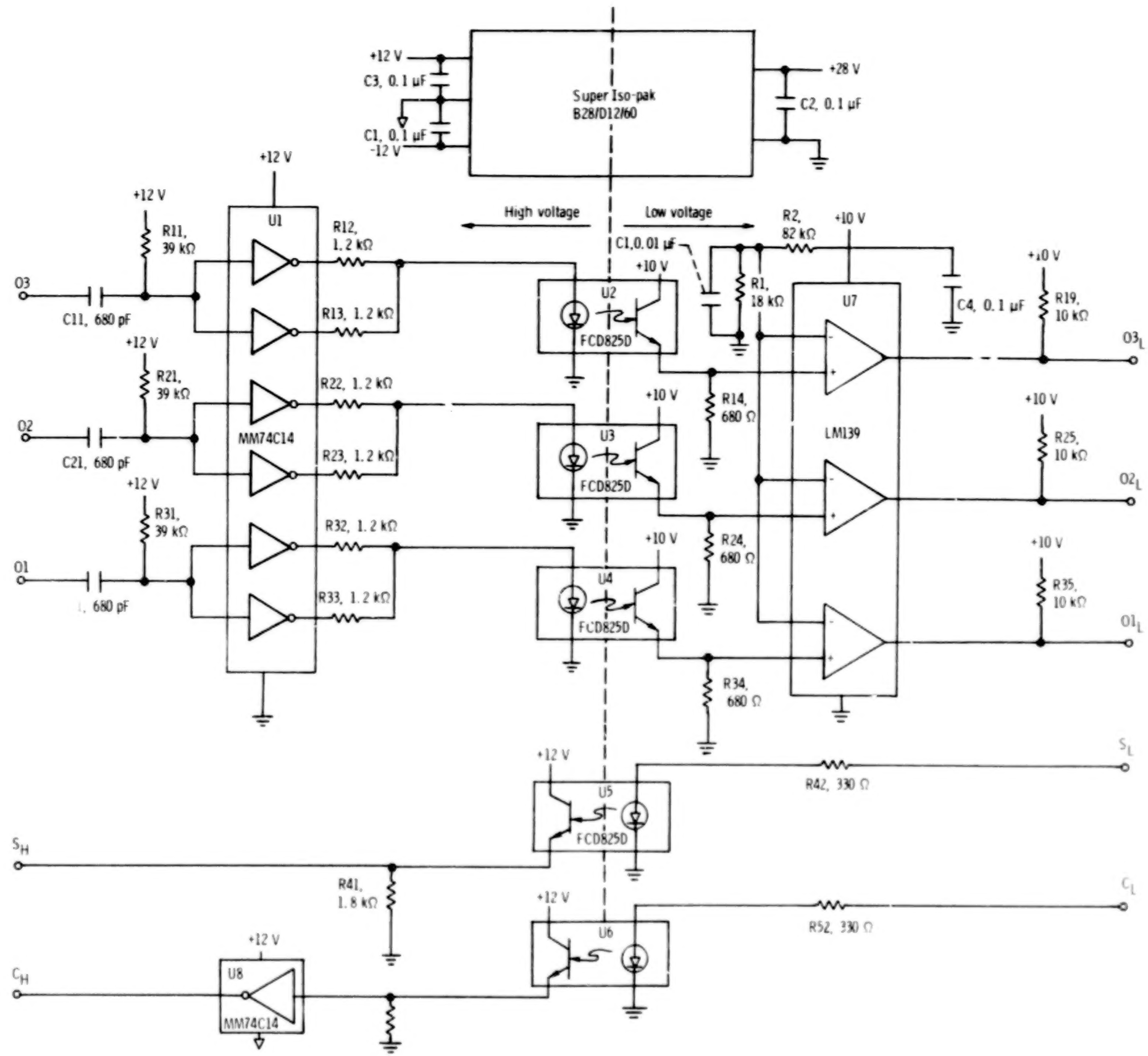


Figure 6. - Optically isolated nanoammeter opto-isolator card.

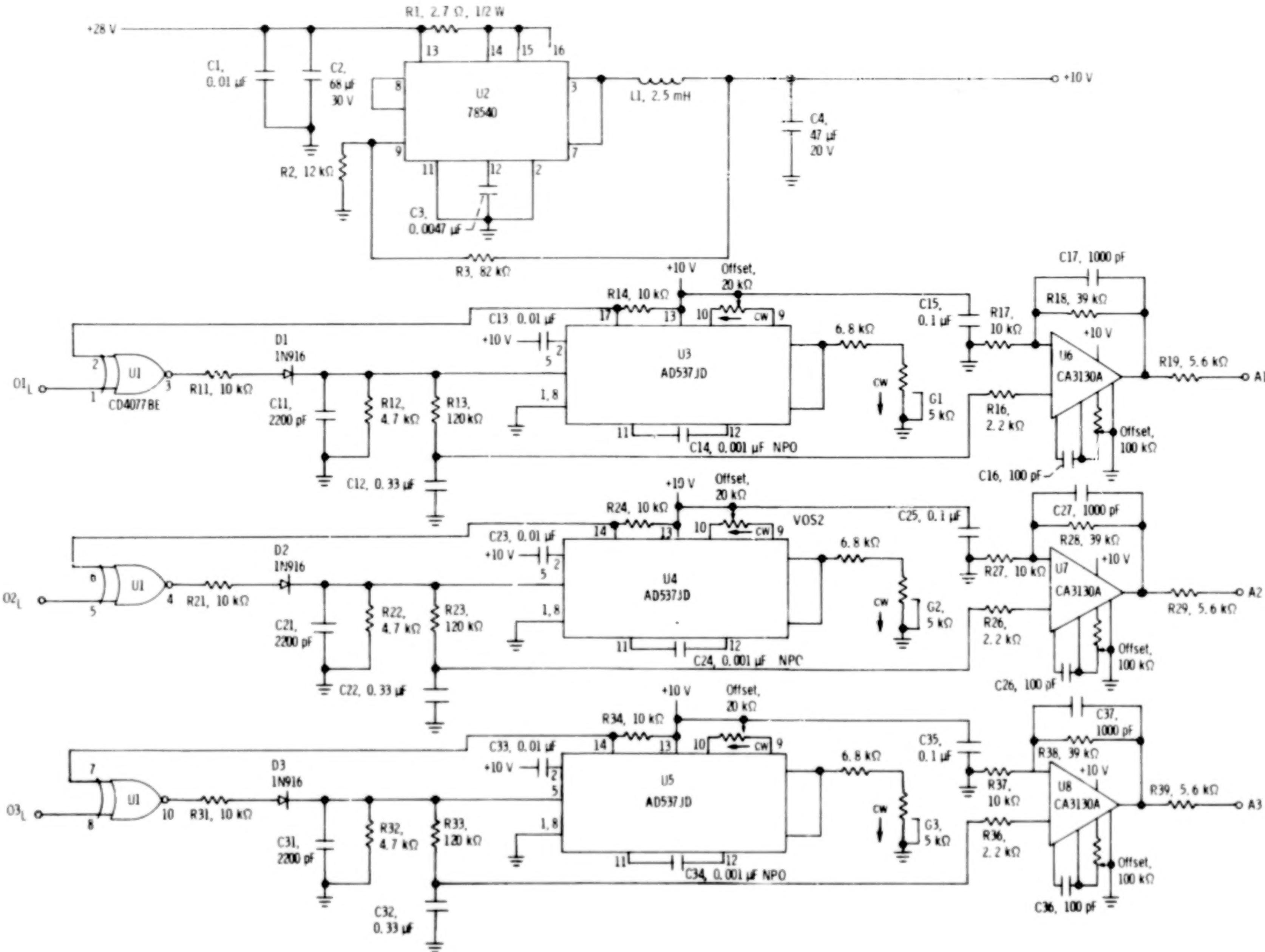


Figure 7. - Optically isolated nanoammeter low-voltage supply and output card.

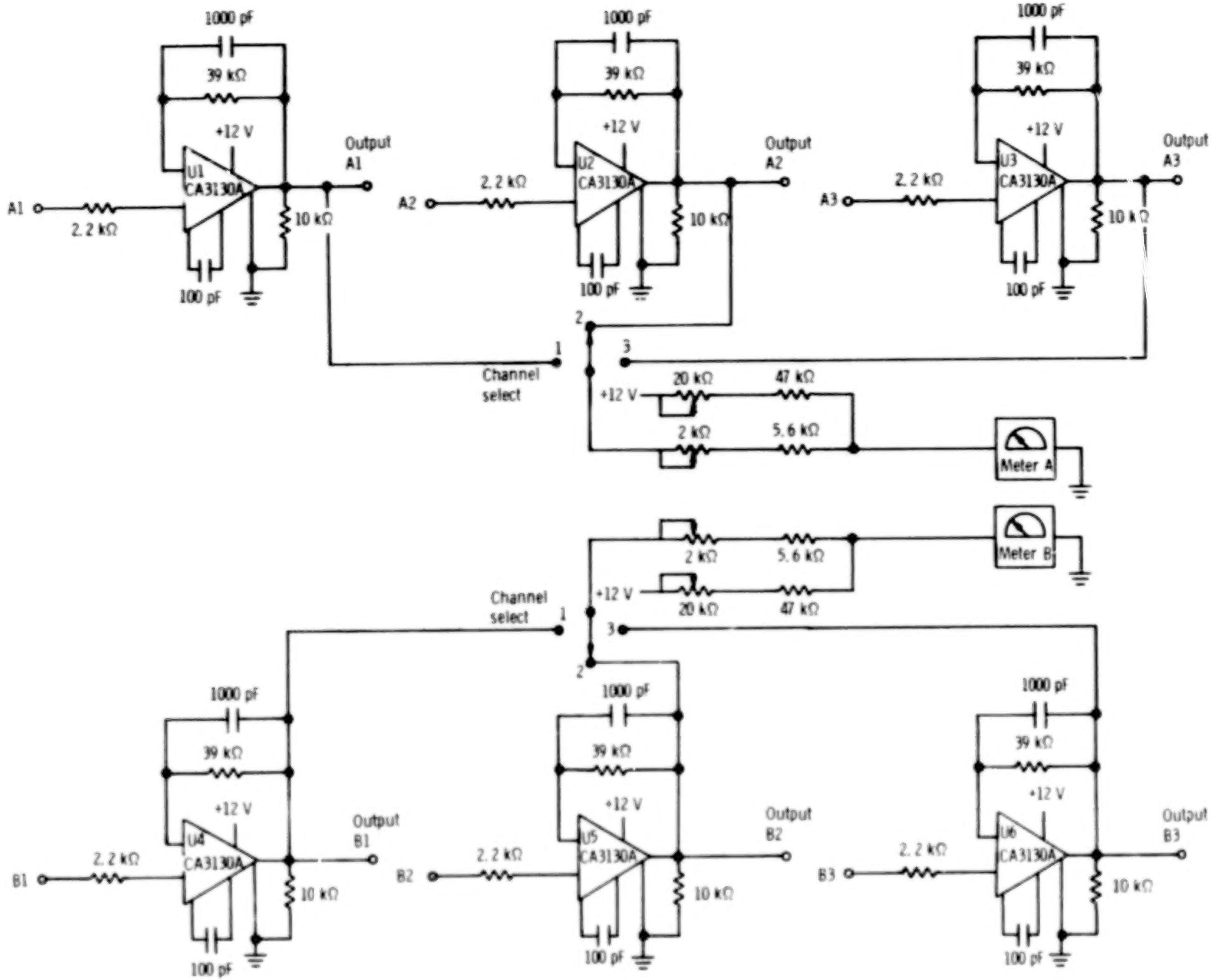


Figure 8. - Control-panel analog signal buffers.

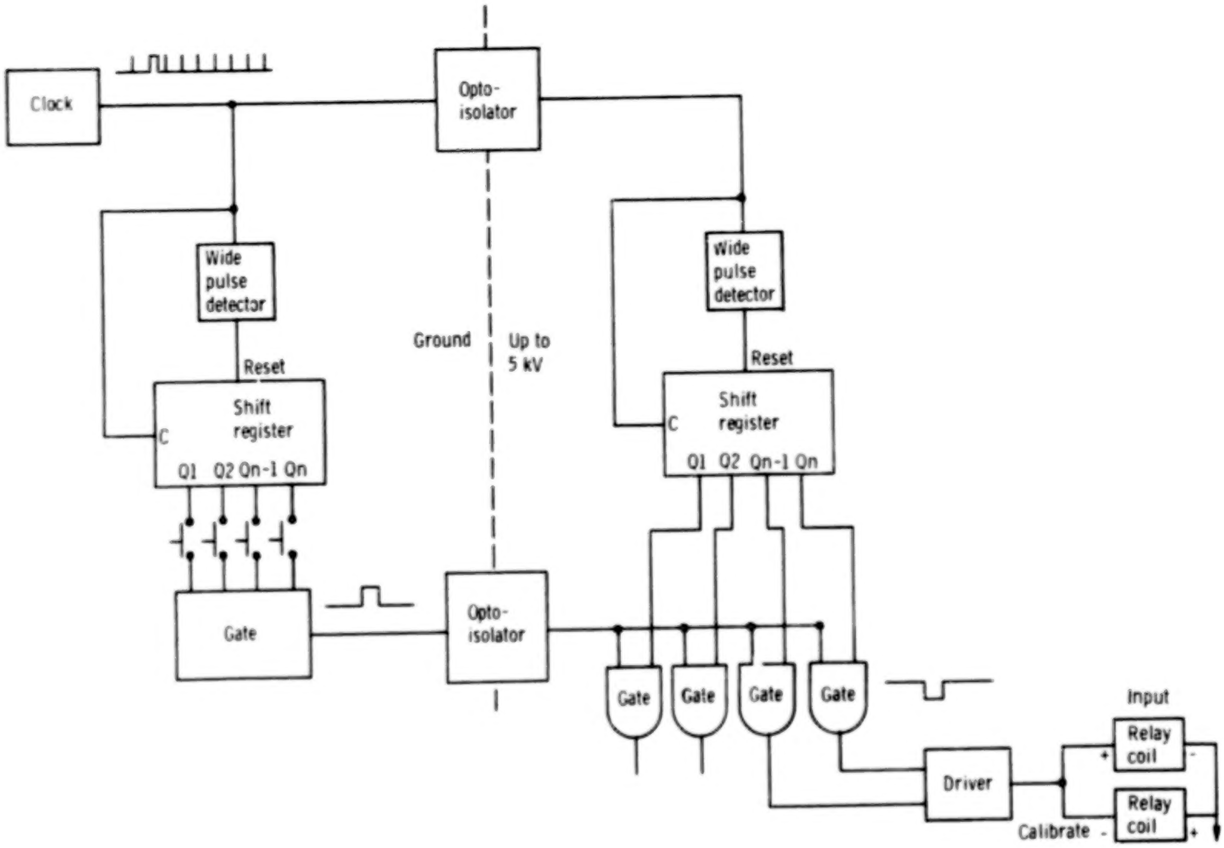


Figure 9. - Optically isolated nanoammeter control block diagram.

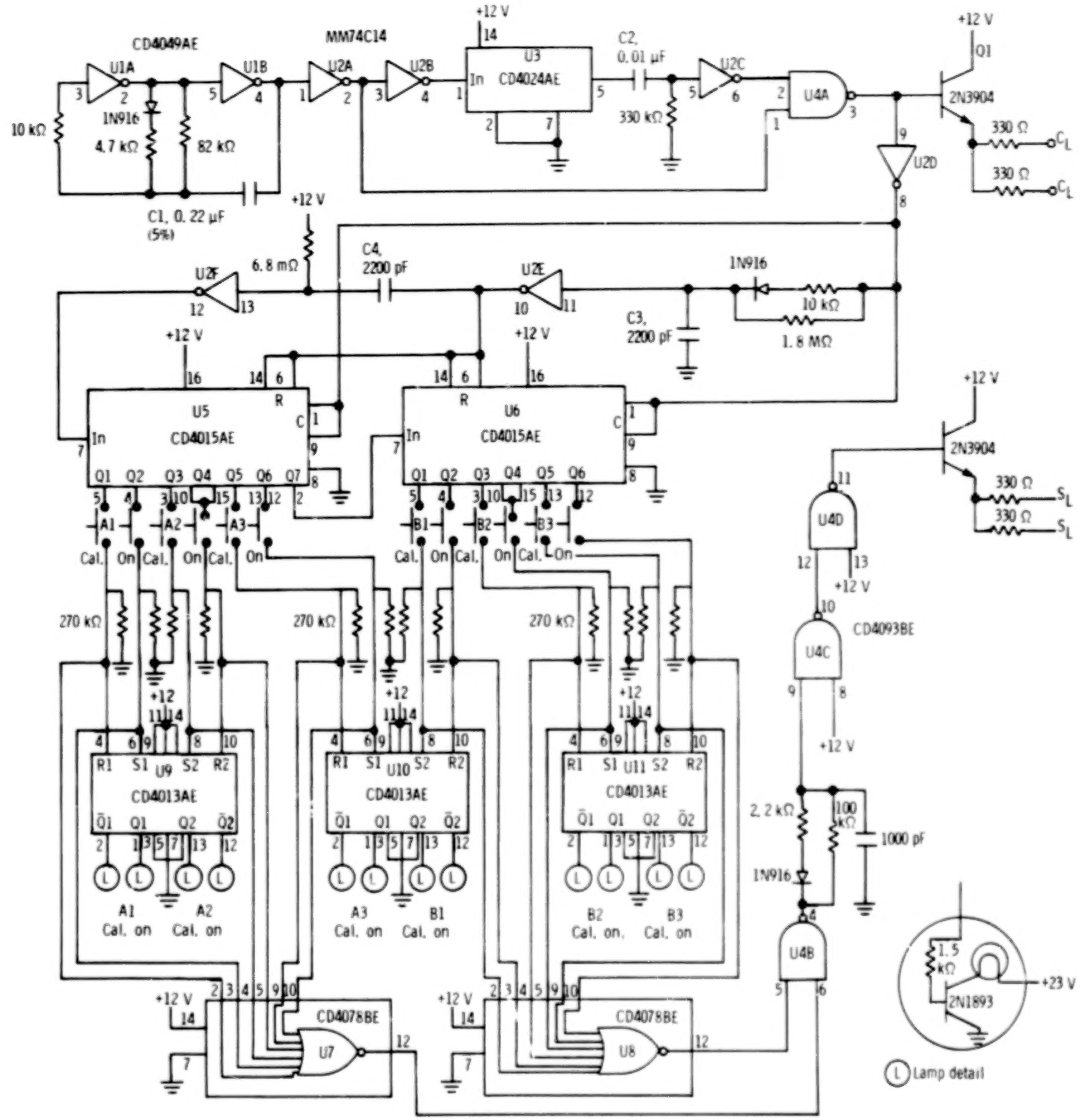

Figure 10. - Control-panel input switch controls.

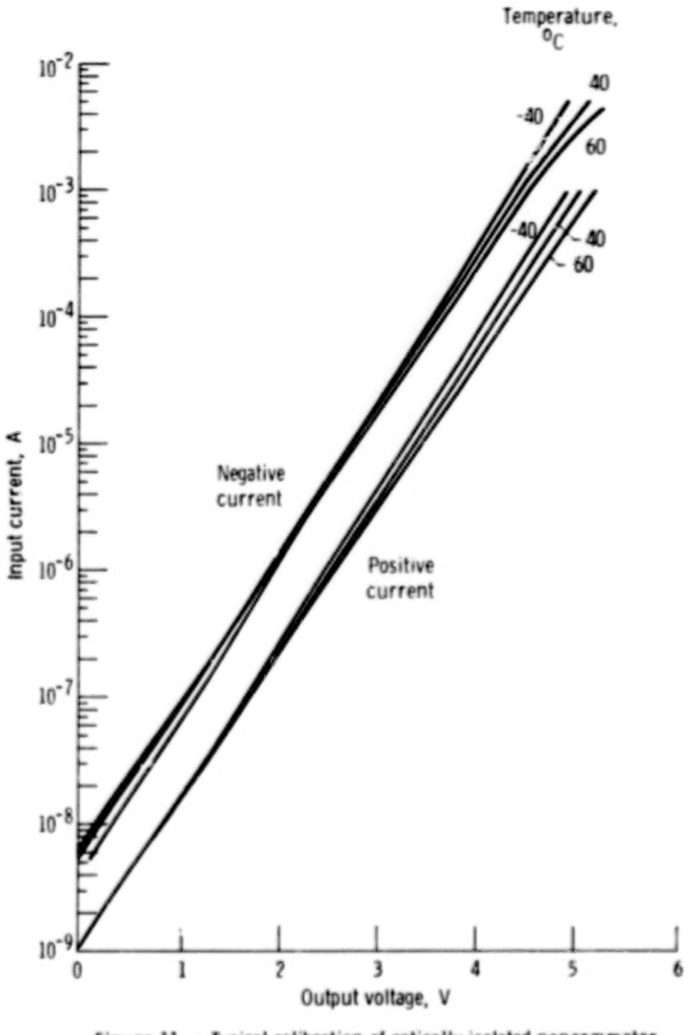


Figure 11. - Typical calibration of optically isolated nanoammeter.

| 1. Report No. | 2. Government Accession No. | 3. Recipient's Catalog No. |
|---|---|---|
| NASA TP-1527 | | |

| 4. Title and Subtitle | 5. Report Date |
|---|---|
| OPTICALLY ISOLATED LOGARITHMIC NANOAMMETER CAPABLE OF FLOATING TO 5 KILOVOLTS | October 1979 |
| | 6. Performing Organization Code |
| 7. Author(s) | 8. Performing Organization Report No. |
| John C. Sturman and John C. DeLaat | E-9934 |
| | 10. Work Unit No. 506-23 |
| 9. Performing Organization Name and Address<br>National Aeronautics and Space Administration<br>Lewis Research Center<br>Cleveland, Ohio 44135 | 11. Contract or Grant No. |
| | 13. Type of Report and Period Covered<br>Technical Paper |
| 12. Sponsoring Agency Name and Address<br>National Aeronautics and Space Administration<br>Washington, D.C. 20546 | 14. Sponsoring Agency Code |

15. Supplementary Notes

16. Abstract

A logarithmic current-measuring instrument has been developed that can operate at a common-mode voltage of 5 kilovolts. Positive or negative currents can be measured from $10^{-9}$ to $10^{-3}$ ampere direct current. Optical isolation is used to control input switching and to provide data referenced to ground potential. Analog meter readouts as well as 0- to 5-volt outputs are provided for peripheral data collection. Six independent channels are provided: Three measure positive currents, and three measure negative currents. This instrument was designed to measure plasma coupling currents as part of the spacecraft environmental interaction studies at the Lewis Research Center. Although designed for vacuum operation, it can be used equally well in air to measure low currents at high common-mode voltages.

| 17. Key Words (Suggested by Author(s)) | 18. Distribution Statement |
|---|---|
| Optical isolation; Isolated; Floating; Nanoammeter; Current measurement; High voltage; Logarithmic | Unclassified - unlimited<br>STAR Category 33 |

| 19. Security Classif. (of this report) | 20. Security Classif. (of this page) | 21. No. of Pages | 22. Price* |
|---|---|---|---|
| Unclassified | Unclassified | 21 | A02 |

* For sale by the National Technical Information Service, Springfield, Virginia 22161

NASA-Langley, 1979

20